GEEA
Research article
Geochemistry: Exploration, Environment, Analysis
Published online July 3, 2015
doi:10.1144/geochem2014-307 | Vol. 15 | 2015 | pp. 361–372

Soil geochemical survey of abandoned mining sites in the Eastern-Central Peloritani Mountains, Sicily, Italy

A. Cosenza[1*], A. Lima[1], R. A. Ayuso[2], N. K. Foley[2], S. Albanese[1], A. Messina[3] & B. De Vivo[1]

[1] Dipartimento di Scienze della Terra, dell'Ambiente e delle Risorse, Università di Napoli Federico II, Via Mezzocannone 8, 80134 Napoli, Italy
[2] U.S. Geological Survey, National Center, Mail Stop 954, Reston, VA 20192, USA
[3] Dipartimento di Fisica e Scienze della Terra, Università di Messina, Viale F. Stagno d'Alcontres 31, 98165 Messina, Italy
* Correspondence: antonio.cosenza@unina.it

Abstract: This investigation focused on topsoils ($n=122$) and vertical profiles ($n=6$) distributed over an area of 250 km^2 in the eastern-central Peloritani Mountains, northeastern Sicily. Georeferenced concentration of 53 elements (including potentially harmful ones), determined by ICP-MS after an aqua regia leach, were used to produce geochemical maps by means of a GIS-aided spatial interpolation process. Results show that there are two distinct areas: the larger, located between the Fiumendinisi, Budali and Ali villages, and the other between C. Postlioni and Femmina Morta, which contain anomalous As (up to 727 mg/kg), Sb (up to 60 mg/kg), Ag (up to 1 mg/kg) and Au (up to 0.1 mg/kg) concentrations. Most of the investigated areas have high contamination levels for As, Zn, Sb, and Pb that exceed the threshold values (As = 20 mg/kg, Zn = 150 mg/kg, Sb = 10 mg/kg and Pb = 100 mg/kg) established for soils by the Italian Environmental Law (Decreto Legislativo 2006, number 152).

The isotopic ratios of $^{206}Pb/^{207}Pb$ and $^{208}Pb/^{207}Pb$ have been measured in selected soils on both leaches [using 1M HNO_3–1.75M HCl (50:50)] and residues thereof. Soil leach reflects possible anthropogenic contamination, whereas soil residues indicate geogenic contributions. Results suggest that most of contamination in the soils is related to the presence of sulphide and sulphosalt rock-forming minerals in the surveyed area. The soil fraction contains a Pb value >1600 mg/kg and has ratios of 1.1695 for $^{206}Pb/^{207}Pb$ and 2.4606 for $^{208}Pb/^{207}Pb$. Only one soil leach isotopic composition could reflect possible anthropogenic contamination. The correlation among As, Zn, Pb contents v. Pb isotopic signatures of $^{206}Pb/^{207}Pb$ indicates that surface and deep soils collected from profiles are dominated by geogenic compositions.

Keywords: Peloritani Mountains; topsoil contamination; Pb isotopic ratios

Received 5 August 2014; **revised** 7 April 2015; **accepted** 5 May 2015

Since ancient times, mankind has sought out the natural resources hosted in the bedrock for economic gain. The principal metals, gold and silver, associated with copper, iron, zinc and lead, are needed by the metallurgic industry. In Italy, the most important centres of mining activities known for Pb, Zn, Cu, Fe, Mn, associated with sulphides of As, Sb, Ag and Au, are located in Sicily, the island of Sardinia and in the Tuscan region.

In Sicily, more precisely in the Peloritani Mountains, there are the well known abandoned mining sites of Val Carbone, Val Pomia, Malonado, San Carlo, Vacco and Migliuso, Budali and Tripi (Fig. 1; De Vivo *et al.* 1993). In the 1960s, mining ended because metal production was no longer economically viable. However, the old mining sites still represent sources of potentially toxic metals affecting the surface environment. In 1999, the Peloritani Mountains were declared a Natural Reserve, where mining is no longer permitted. The assessment of environmental pollution in this portion of the Peloritani Mountains, using Pb isotopes as a tool to discriminate geogenic concentrations from nearby industrial activities, was dictated by the concerns of people living in the villages near the industrial sites.

A regional stream sediment geochemical survey (De Vivo *et al.* 1993; Fig. 1, box A) identified diffuse Au anomalies along with anomalies of As, Hg, Sb, Zn and Pb. A follow-up stream sediment survey (De Vivo *et al.* 1993, 1998*a*), focused on a smaller area (Fig. 1, box B), confirmed the occurrence of Au anomalies and showed that they are distributed in a belt along the thrust contact of two different Hercynian metamorphic units (Fig. 2). Figure 2 shows historic mining sites that were mined at a small scale for Pb, Zn and Cu associated with sulphides and sulphosalts of Fe, Mn, As, Sb, Ag and Au (Ferla & Meli 2007, and references therein; Saccà *et al.* 2003, 2007, and references therein). Also shown in Figure 2 are known metal sulphide mineralized areas near Mandanici, Fiumedinisi and Bafia (De Vivo 1982; Bonardi *et al.* 1982).

The purpose of this study was to: (1) assess contamination levels in an area affected by high concentrations of toxic elements in soil caused both by the occurrence of sulphide minerals and historic mining activities; and (2) evaluate geogenic v. anthropogenic soil contamination using Pb isotope analysis.

Study Area

The geographic domains of the Peloritani Mountains and Eastern Nebrodi Mountains (NE Sicily, Italy), which are characterized by high relief traversed by short, seasonal rivers and torrents, geologically form the Peloritani Chain. These mountains extend for *c.* 100 km (Fig. 1). The study area (Fig. 2) is sparsely populated and the population is concentrated in villages close to the seasonal rivers.

The Peloritani Chain constitutes the southernmost portion of the Calabria-Peloritani Arc, which is an arc-like structure connecting the NW–SE-trending Italian Apennines with the east–west-trending Sicilian and North Africa Maghrebis. It is formed by a stack of continental and oceanic crust units structured in the Tertiary (Amodio-Morelli *et al.* 1976; Bonardi *et al.* 1996, 2004; Messina

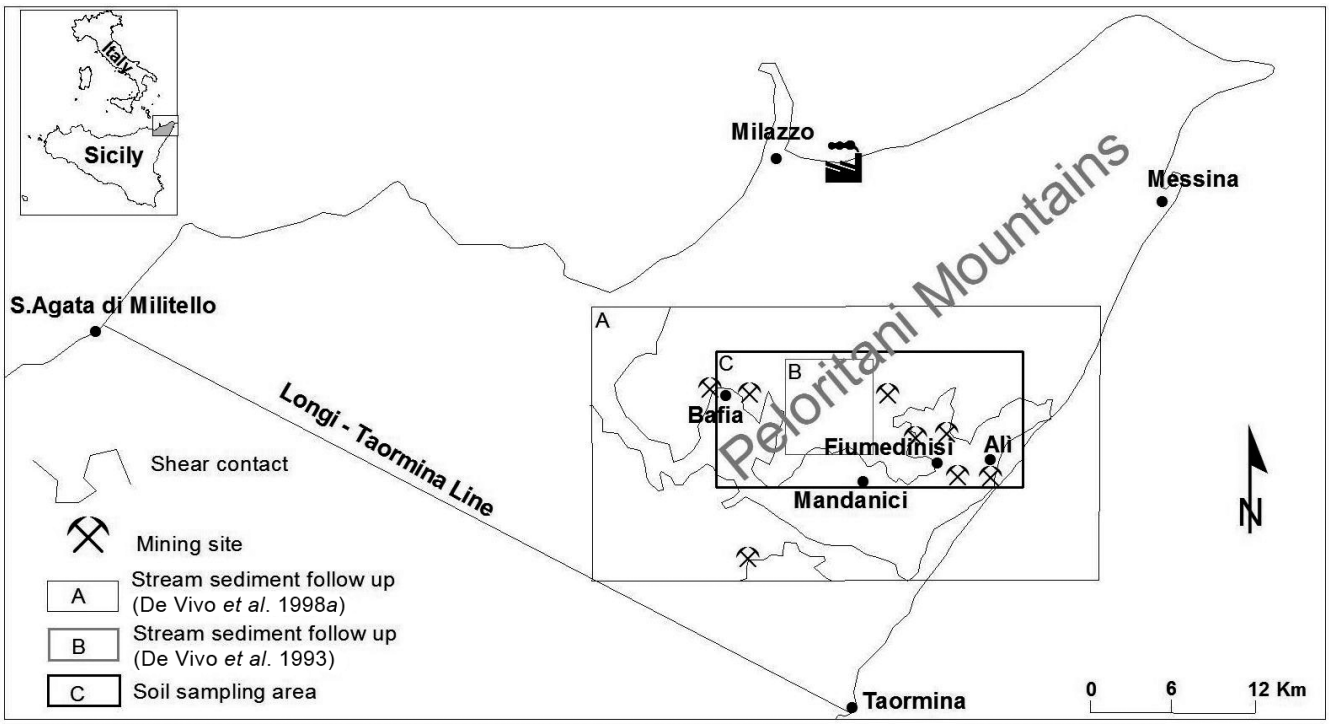

Fig. 1. A general view that shows the previous stream sediment study area (box A and B) (De Vivo *et al.* 1993, 1998*a*) and the current study area (box C) on the island of Sicily, Italy. Also shown is the shear contact between Aspromonte, Mandanici and Fondachelli units (De Vivo *et al.* 1993).

1996). According to the current view, the continental units were derived from the Jurassic-Cretaceous Mesomediterranean Microplate whereas the oceanic units originated from the Tethys Ocean branches located between this microplate and the main plates (Guerrera *et al.* 1993; Martín-Algarra *et al.* 2000; Somma *et al.* 2005*a*,*b*; Perrone *et al.* 2006). The Peloritani Chain consists of a stack of continental crust units involving Pan-African and Variscan crystalline basements and remnants of original Meso-Cenozoic sedimentary cover rocks. Basements and covers are locally affected by an Alpine overprint (Messina *et al.* 1990, 2004; Atzori *et al.* 1994; Bonardi *et al.* 2008). The Pan-African basements derive from a crystalline Proterozoic crust, whereas the Variscan basements originate from Palaeozoic sedimentary-volcanic sequences underwent to different stages of Variscan metamorphic processes (Messina *et al.* 2004, 2013; Carbone *et al.* 2008, 2011).

The structural setting of the Peloritani Chain involves nine Alpine tectonic units, which from top to bottom are: Aspromonte, Mela, Piraino, Mandanici, Alì, Fondachelli, San Marco d'Alunzio, Longi-Taormina and Capo Sant'Andrea units (Carbone *et al.* 2008, 2011). The Alpine units outcropping in the area of investigation include Aspromonte, Mela, Piraino, Mandanici and Alì units (Fig. 2).

The Aspromonte unit consists of a Palaeo-Proterozoic crystalline (plutonites and metamorphites) basement, affected by a Pan-African HT granulite facies metamorphism, intruded by a Late-Pan-African orogenic peraluminous plutonites, followed by a Variscan LT granulite to LT amphibolite facies re-equilibration, with intrusion of Late-Variscan orogenic plutonites. Pre-Variscan and Late-Variscan rocks were also locally affected by an Alpine MHP greenschist to amphibolite facies metamorphic overprint (Messina *et al.* 1990, 2004, 2013; De Gregorio *et al.* 2003; Micheletti *et al.* 2007; Bonardi *et al.* 2008; Carbone *et al.* 2008, 2011). Where exposed, the unit consists of gneisses, schists, amphibolites, metahornblendites metapyroxenites, metaperidotites (intraplate tholeiites; Macaione *et al.* 2010), silicate marbles, quartzites, intermediate to acidic orthogneisses, peraluminous leucotonalites to leucomonzogranites, pegmatites and aplites (Carbone *et al.* 2008, 2011; Fig. 2).

The Mela unit crops out extensively in the studied area where it is interposed between the overlying medium- to high-grade Aspromonte unit and the underlying low- to medium-grade Piraino unit or, rarely, the Mandanici unit. The unit consists of basement made up of a Palaeozoic sedimentary-volcanic sequence interested by an Eo-Variscan eclogite facies metamorphism (Compagnoni *et al.* 1998), and by a Variscan Barrovian-type LT amphibolite to HT greenschist facies re-equilibration (Messina *et al.* 1997). The basement is made up of Grt-relict paragneisses and micaschists with large static blastesis of Hercyno-type minerals, thick layer marbles including lenses of Grt-relict anphibolitized eclogites (Messina *et al.* 2004, 2013; Carbone *et al.* 2008, 2011; Fig. 2).

The Piraino unit (Messina *et al.* 1998) is sandwiched between the overlying Mela or Aspromonte units and the underlying Mandanici unit. It consists of a Palaeozoic basement made up of a sedimentary-volcanic sequence affected by a Variscan metamorphic prograde zone, which ranges from the chlorite zone of the greenschist facies to the staurolite-oligoclase zone of amphibolite facies. The unit preserves slices of an Upper Triassic–Aalenian sedimentary cover (Cecca *et al.* 2002). In the study area the basement comprises dark graphite-garnet phyllites, metarenites, amphibolite schists and quartzites (Fig. 2).

The Mandanici unit (Ogniben 1960) occurs between the overlying Piraino, Mela or Aspromonte units, and the underlying Ali or Fondachelli units. It consists of a Palaeozoic sedimentary-volcanic sequence affected by a Variscan metamorphic prograde zone from LT greenschist facies to the beginning of amphibolite facies (oligoclase+almandine). Several slices of an Upper Triassic–Lower Liassic cover, with typical yellow gypsum-rich evaporates and cargneules, are also present. The basement is made up of green, silver and lead-coloured phyllites and metarenites, actinolitic amphibolite schists, quartzites and marbles (Messina *et al.* 2004, 2013).

The Alì unit (Caire *et al.* 1965) crops out along the Alì-Montagnareale alignment. In the studied area, the Aspromonte and Mela units tectonically rest upon the Alì Unit (Modderino klippe) (Atzori 1968; Carbone *et al.* 2008). The unit consists of a Palaeozoic basement made up of sedimentary sequence (Lower

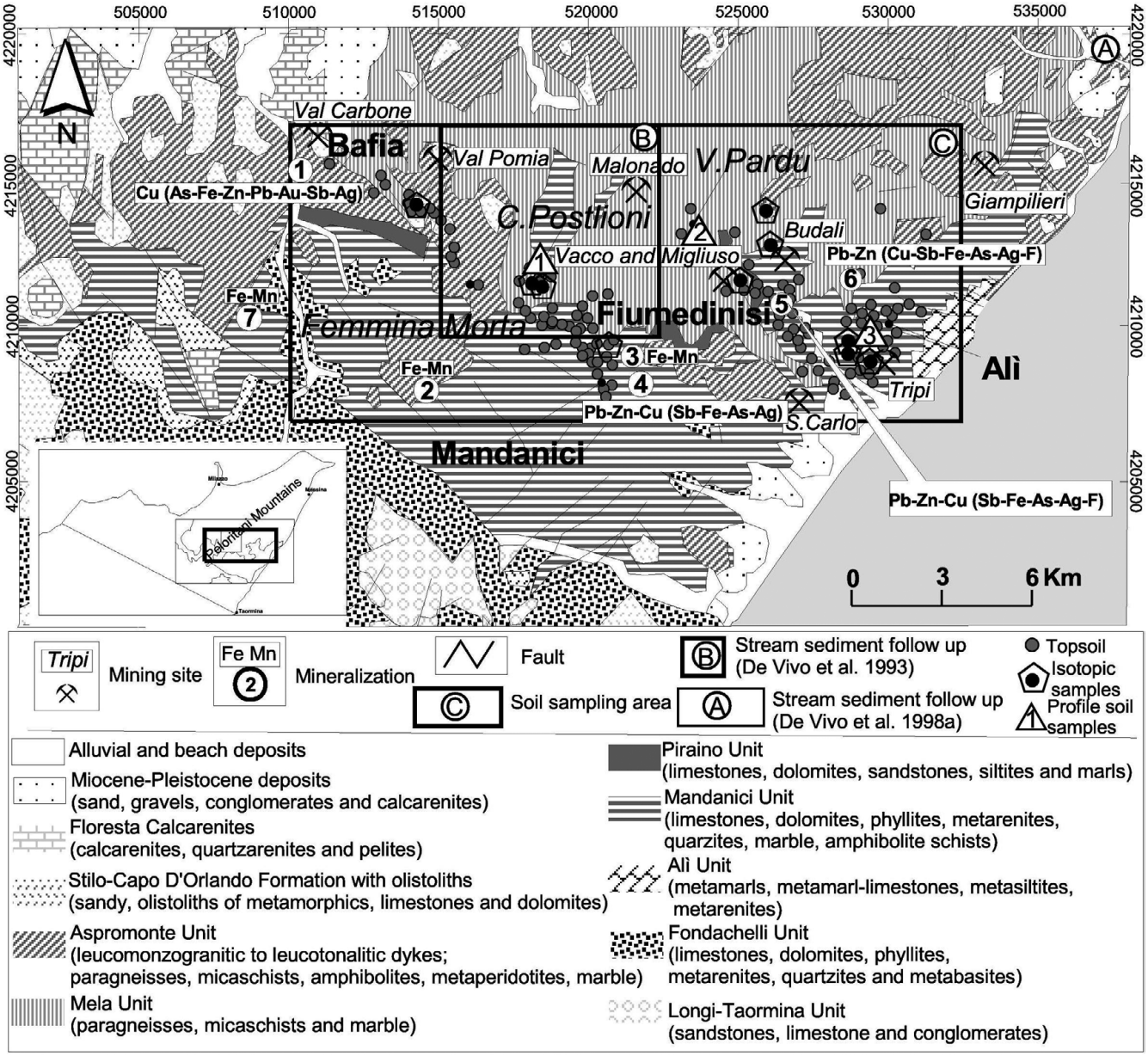

Fig. 2. Geological sketch map together with topsoil sampling sites, topsoil sites selected for Pb isotopic ratio study and soil profile sites. Also shown are known areas of Pre-Alpine stratabound mineralization (Bonardi *et al.* 1982 and De Vivo 1982; named: 1 Bafia, 2 Raiù, 3 Pizzo Barramanco, 4 Mandanici, 5 Mandanici, 6 Fiumedinisi, 7 Alì) and the names of old mining sites (De Vivo *et al.* 1993). For boxes A, B and C, see Figure 1.

Carboniferous-Devonian; De Stefani 1911) affected by a very-low grade Variscan metamorphism, and a Mesozoic sedimentary cover. Basement and cover were overprinted by an Alpine MLT sub-greenschist facies metamorphism. The basement comprises only metasiltites and metarenites; the cover is made up of continental red bed, cargneules, marls, limestones and siltites (Somma *et al.* 2005*a*; Carbone *et al.* 2008).

Mineralization

In the Peloritani Mountains, sulphide-mineralized rocks are widespread in all the basement units. They occur most commonly as stratabound and stratiform layers, veins, and lenses. Mineralized hydrothermal breccias are common along the Alpine shear planes, in the almost sub-horizontal thrust contacts (Fig. 2), and in the Plio-Pleistocene fault systems where sulphide minerals also occur in late veins and fractures.

Previous studies of mineral resources of the Peloritani Mountains by De Vivo (1982), De Vivo *et al.* (1993, 1998*a*) and Bonardi *et al.* (1982) indicated the occurrence of metal sulphide (Pb, Zn, Cu, Sb, Fe, As, F, Ag and Au) mineralization near Mandanici, Fiumedinisi and Bafia (Fig. 2).

The historic mines (Fig. 2) exploited mainly stratabound ore deposits associated with quartz-fluorite gangue, galena or pyrite-bearing massive layers in Variscan phyllites or along discordant veins. Such occurrences are clearly shown by geochemical anomalies from a regional survey carried out in the Peloritani Mountains (Fig. 1, box A) both on rocks and stream sediments in the period 1987–1991 by RIMIN SpA (belonging to the State Co ENI – Ente Nazionale Idrocarburi). The geochemical database resulting from this study has been used to compile geochemical maps at a regional scale (De Vivo *et al.* 1998*b*), which have been instrumental in designing a later follow-up stream sediment survey in a selected area (Fig. 1, box B) characterized by the occurrence of Au anomalies (De Vivo *et al.* 1993, 1998*a*).

High Au anomalies (up to 3300 μg/kg) occur near the Mandanici and Fiumedinisi (Au up to 726 μg/kg) areas and high Ag (200 μg/kg) contents near Bafia. Additionally, high As, Pb, Sb, Zn and Cu

anomalies correspond to the old mines of S. Carlo and Tripi, in the area between Alì and Fiumedinisi.

Although the primary source of Au anomalies remains speculative, they are interpreted to be related to primary Proterozoic plutonic and Palaeozoic volcanogenic activity; Au was later remobilized during metamorphic processes (Pan-African, Variscan and Alpine processes in the Aspromonte unit and Variscan processes in the other units; Messina *et al.* 2004, 2013; Carbone *et al.* 2008, 2011), and ultimately deposited along the Alpine overthrust contact (Fig. 1) between the Aspromonte, Mela and Mandanici units (De Vivo *et al.* 1993, 1998*a*).

Methods

Topsoil survey and soil profile samples

Because of the rough terrain, the area could not be sampled using a uniform sampling grid. Figure 2 shows the locations of 122 topsoil sampling sites distributed over 250 km^2. The topsoils were collected from the surface to a depth of 15 cm, following the protocol of the FOREGS (Forum of European Geological Surveys) program (Plant *et al.* 1996; Salminen *et al.* 1998). A second soil sampling was also conducted to obtain three detailed soil profiles. The profiles collected soils down to a depth of 1 m (Fig. 2). In each soil profile, two soil samples were collected: one at the top (0–20 cm) and one at the bottom (80–100 cm) of the profile, for a total of six soil samples across the three profiles. All soils were dried under infrared light with a maximum temperature of 37°C, and sieved to retain the <100-mesh fraction (150 µm) for analysis.

Analysis and statistical data

Chemical analyses were carried out at Acme Analytical Laboratories Ltd (Vancouver, Canada), by ICP-MS using Acme's Group 1F-MS package (modified aqua regia digestion, 1:1:1 mixture of reagent grade HCl, HNO_3 and H_2O) for 53 elements. The final database on which to carry out the statistical analysis is composed of 40 elements. Thirteen elements have not been considered, either because most of samples had values below by instrumental detection limits [(Ge, Hf, Ta, Re, In, Pd, Pt) or very close (B, Nb, Sr, U, Y, W)]. The precision and accuracy of analysis are in the range of 15% (Table 1) with the exception of a few elements. Table 2 shows the statistical parameters of the analysed soil. Figure 3 shows the statistical frequency data for As, Zn, Sb, Pb, Cd, Hg, Sn and V. The limit recommended by Italian Environmental Law (D. Lgs 152/06) for residential and recreational area land use (Residential Action Limit – RAL) and industrial/commercial land use action limit (IAL) are represented in Table 3.

Geochemical mapping

The geochemical maps in Figures 4 and 5 have been obtained following the multifractal inverse distance weighted (MIDW) interpolation method, with intervals reclassified by means of the concentration–area fractal method (Cheng 2003; Xu & Cheng 2001; Lima *et al.* 2003).

Isotopic analysis

In order to characterize the mineralized areas, seven galena concentrates were collected from old mining sites at Vacco and Migliuso, Budali, and Tripì. The galenas were analysed for their Pb isotopic compositions (Fig. 2).

Lead isotopic compositions were also measured from selected soil samples from profiles ($n=6$; their location shown in Fig. 2) using a thermal ionization mass spectrometer (Spectromat-Finnigan-Mat 262; Ayuso *et al.* 2008) at the U.S. Geological Survey (Reston, VA, USA). Approximately 2 g of undisturbed soil sample were prepared for isotopic analysis using a step-leaching procedure.

Table 1. *Accuracy and precision for 40 elements in topsoils*

Element	Accuracy (%)	%RPD*
Al	16.27	1.25
Ca	10.22	6.21
Fe	6.49	2.1
K	16.48	4.72
Mg	3.81	2.76
Na	13.84	5.72
P	2.19	4.86
S	8.33	0.01
Ti	10.08	8.10
As	11.46	3.75
Ba	18.7	4.45
Be	6.25	12.21
Bi	5.27	4.54
Cd	3.92	5.06
Ce	2.7	4.37
Co	6.63	12.49
Cr	19.62	3.45
Cs	6.87	3.58
Cu	5.02	3.19
Ga	14.67	2.82
La	16.14	4.35
Li	19.62	5.00
Mn	6.3	3.05
Mo	2.53	3.36
Nb	13.38	7.79
Ni	0.27	2.71
Pb	5.28	3.84
Rb	10.82	8.32
Sb	4.48	5.83
Se	5.00	18.71
Sn	3.24	9.37
Te	7.18	10.55
Th	8.52	4.73
Tl	0.78	10.57
V	0.29	2.78
Zn	3.69	4.24
Zr	6.48	12.16
Ag	6.74	8.13
Au	11.29	11.84
Hg	3.63	9.44

*Relative Percent Difference is used to calculate the precision from duplicate measurements.

The samples were leached using a 1-ml mixture of 1M HNO_3–1.75M HCl (50:50), placed in an ultrasonic bath (at 35°C) for 2 h and left to equilibrate overnight. Samples were then centrifuged for 5 min at 5000 rpm producing a leachate ('L', one step-leaching procedure) and a residue fraction (Residue, 'R'). The two fractions were then evaporated and processed using the following sequence of ultrapure acid dissolution: concentrated HNO_3, concentrated HF, 4M HCl and 0.5M HBr (Ayuso *et al.* 2013). The samples were loaded in HBr form in the column. A second pass of the ion-exchange columns ensured the purity of the Pb solution extracted.

All the reagents were sub-boiled in a two-bottle Teflon still at a temperature of 80°C to reduce the Pb blanks. The galena samples were cleaned with 20 ml of 2M HCl placed in a beaker on hot-plate with the temperature below 100°C. The white salt formed on the bottom of beakers was purified with 5 ml of 4M HCl. The Pb collected through these procedures for each analysed sample was loaded on a single Ta rhenium degassed filament using the classic method of silica gel and phosphoric acid, and isotopic data were collected in a static running mode. The ratios obtained were corrected for mass fractionation relative to the NIST- SRM981 standard (Ayuso *et al.* 2008). The isotopic results are reported in Tables 4 and 5.

Table 2. *Geochemical data, detection limits (DL) of 40 selected elements*

Elements	DL	Range	Mean	Geo Mean	Std Dev	25%ile	50%ile	75%ile	95%ile	Uncultivated* soils average
Al (%)	0.01	0.28–8.16	2.63	2.40	1.05	2.04	2.46	3.07	4.20	1.6–6.5
Ca (%)	0.01	0.06–18.1	1.12	0.70	1.99	0.36	0.69	1.12	2.62	
Fe (%)	0.01	1.05–6.97	4.38	4.30	0.99	3.90	4.39	4.82	6.22	0.47–4.3
K (%)	0.01	0.07–1.37	0.32	0.30	0.22	0.17	0.24	0.39	0.73	
Mg (%)	0.01	0.15–10.5	1.21	1.00	1.06	0.81	1.07	1.39	1.89	
Na (%)	0.001	0.007–0.312	0.05	0.04	0.04	0.03	0.04	0.06	0.10	
P (%)	0.001	0.012–0.306	0.11	0.10	0.05	0.08	0.11	0.12	0.20	
S (%)	0.02	0.015–0.31	0.06	0.05	0.05	0.03	0.04	0.07	0.13	
Ti (%)	0.001	0.003–0.327	0.07	0.04	0.07	0.02	0.05	0.10	0.19	0.17–0.66
As (mg/kg)	0.1	1.3–726	84	41.5	122	19.6	32.7	95.1	261	6.7–13
Ba (mg/kg)	0.5	16.4–973	144	118	117	81.2	117	166	337	
Be (mg/kg)	0.1	0.2–2.3	0.90	0.80	0.42	0.60	0.80	1.08	1.80	0.76–1.3
Bi (mg/kg)	0.02	0.05–1.42	0.48	0.40	0.22	0.34	0.43	0.56	0.91	
Cd (mg/kg)	0,01	0.02–11.2	0.48	0.20	1.26	0.15	0.24	0.41	0.78	0.1–0.7
Ce (mg/kg)	0.1	6.9–243	67.5	56.5	41.7	37.1	56.7	82.6	144	
Co (mg/kg)	0.1	5.6–62	24.9	23	9.65	20.7	25.1	28	38.8	1–14
Cr (mg/kg)	0.5	4–105	42.9	38.6	19.1	29.7	38.5	51.1	81.6	11–78
Cs (mg/kg)	0.02	0.54–13.6	2.71	2.3	1.79	1.58	2.21	3.36	5.8	
Cu (mg/kg)	0.01	6.49–169	62.8	57.6	25.3	47.1	59.8	75.5	103	8.7–33
Ga (mg/kg)	0.1	0.7–20.1	8	7.41	3	6.12	7.45	9.8	13.1	
La (mg/kg)	0.5	3.3–129	32.9	27.9	20.1	19.1	28.2	39.7	66.5	
Li (mg/kg)	0.1	5.3–111	42.8	38.3	19.4	31.5	41.3	49.9	85.2	
Mn (mg/kg)	1	170–5518	924	808	664	600	789	1042	1625	60–1100
Mo (mg/kg)	0.01	0.19–4.38	1.21	1.10	0.58	0.85	1.10	1.44	2.10	0.2–5
Nb (mg/kg)	0.02	0.09–11.5	2.34	1.40	2.49	0.68	1.41	2.81	8.60	
Ni (mg/kg)	0.1	10.7–135	48.1	44.4	17.9	40.1	48.3	56.1	72.8	4.4–23
Pb (mg/kg)	0.01	6.67–1658	65.8	37.6	160	22.5	35.4	47.5	144	2.6–25
Rb (mg/kg)	0.1	3.6–150	25.3	19.9	20.3	11.5	17.8	33.1	52.9	
Sb (mg/kg)	0.02	0.1–60.7	7.62	1.90	12.2	0.44	1.31	9.06	32.2	2.0
Se (mg/kg)	0.01	0.1–2.9	0.75	1.20	0.45	0.50	0.60	0.80	1.60	0.27–0.73
Sn (mg/kg)	0.1	0.2–14.5	1.58	53.9	1.62	0.70	1.20	2	3.20	3–10
Te (mg/kg)	0.02	0.015–0.33	0.07	0.06	0.05	0.04	0.06	0.08	0.16	
Th (mg/kg)	0.1	1.1–33.1	9.60	8.30	5.41	6.23	8.05	11	19.4	
Tl (mg/kg)	0.02	0.04–10	0.52	0.28	1.03	0.14	0.26	0.58	1.49	
V (mg/kg)	2	11–132	54.6	48.8	26.3	35	46.5	68.5	104	15–110
Zn (mg/kg)	0.1	23.4–5363	241	130	614	84.8	115	154	411	25–67
Zr (mg/kg)	0.1	0.2–17.3	3.15	1.93	3.76	1.10	1.50	3.28	13.4	
Ag (μg/kg)	2	16–1107	115	80.7	142	47	72	120	336	
Au (μg/kg)	0.2	0.2–100	10.7	5.60	14.9	2.53	5.35	10.4	37.8	
Hg (μg/kg)	5	3.7–1564	169	73.4	268	28.5	67.5	221	639	45–160

*Uncultivated soils average from Connor & Shacklette (1975) and Shacklette & Boerngen (1984).

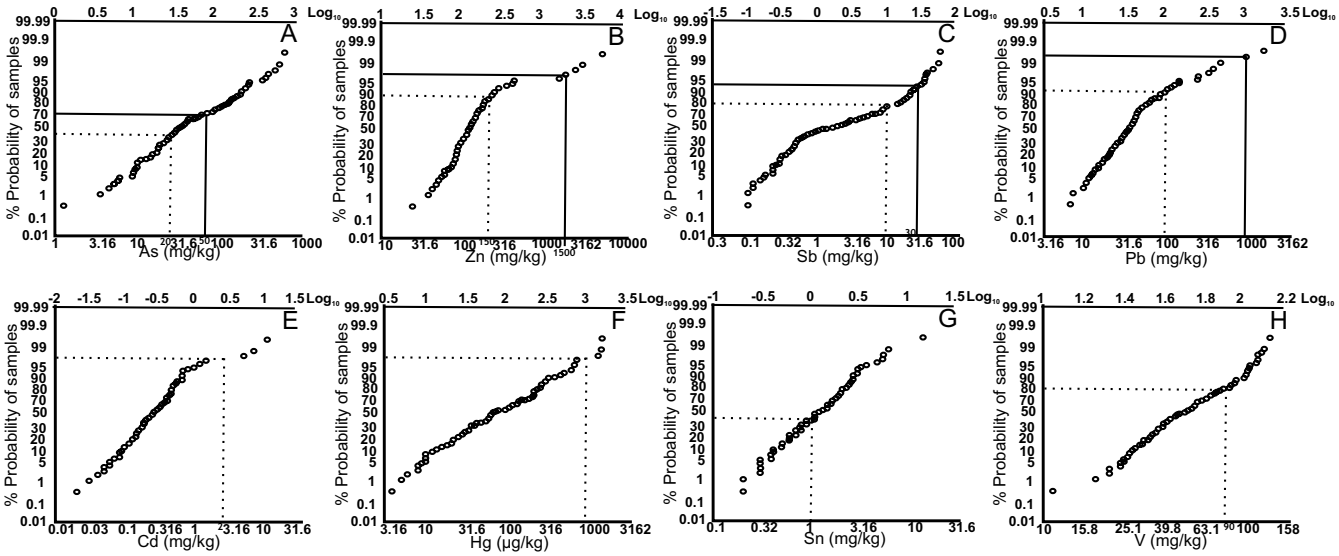

Fig. 3. Cumulative frequency curves for selected potentially toxic elements As, Zn, Sb, Pb, Cd, Hg, Sn and V (A–H). Also shown is the percentage cumulative value corresponding to the RAL (continuous orange line) and to the IAL (continuous red line).

Table 3. *Intervention limits in mg/kg for soil as defined by Italian Environmental Law (152/06) for Residential Action Limit (RAL) and Industrial/Action Limit (IAL)*

Element	RAL	IAL
As	20	50
Be	2	10
Cd	2	15
Co	20	250
Cr	150	800
Cu	120	600
Hg	1	5
Ni	120	500
Pb	100	1000
Sb	10	30
Se	3	15
Sn	1	350
Tl	1	10
V	90	250
Zn	150	1500

Results

Frequency statistical data for topsoils

The Italian Environmental Law (D. Lgs 152/06) fixed two limits, one for residential and recreational land use (Residential Action Limit, RAL) and the second one for industrial/commercial land use (Industrial Action Limit, IAL), for 15 toxic elements comprising As, Be, Cd, Co, Cr, Cu, Hg, Ni, Pb, Sb, Se, Sn, Tl, V and Zn for topsoils (Table 3). Figure 3 reports the cumulative frequency contents of As, Zn, Sb, Pb, Cd, Hg, Sn and V in the 122 topsoils.

Arsenic, Zn, Sb and Pb exceed both the RAL and IAL limits (Fig. 3A–D). Cadmium, Hg, Sn and V exceed only the RAL limit (Fig. 3E–H).

Distribution of geochemical data

The geochemical map for As in topsoils (Fig. 4A) shows values in the of range 1.3–727 mg/kg, with a mean value of 84 mg/kg (Table 2). It shows minimum values close the village of Bafia and in the northeastern zone of Alì (1.3–21 mg/kg). Most of the values exceed both the limits fixed by law (RAL = 20 mg/kg and IAL = 50 mg/kg; Table 3).

The contents of Zn in topsoils range between 23 and 5363 mg/kg, with a mean value of 241 mg/kg (Table 2). The geochemical map represented in Figure 4B shows that the areas of high distribution of Zn are located between C.Postlioni and Femmina Morta and between Fumedinisi and Ali territories. Again, both the legal limits for Zn (RAL = 150 mg/kg and IAL = 1500 mg/kg) are exceeded (Table 3).

The Sb geochemical map for topsoils (Fig. 4C) shows values in the range of 0.1–60 mg/kg, with a mean value of 7.62 mg/kg (Table 2). High values (up to 60 mg/kg) occur in the area between Fiumedinisi and Alì, reflecting the presence of sulphide mineralization at old mining sites. Both legal limits for Sb (RAL = 10 mg/kg and IAL = 30 mg/kg) are exceeded (Table 3).

The Pb contents in the topsoils fall in a range of 6.7 to 1658 mg/kg, with a mean 65.9 mg/kg (Table 2). High Pb values are concentrated in a small area north and south of Alì (100–480 mg/kg) and C. Postlioni (480–1658 mg/kg) (Fig. 4D). Most of the studied area falls in the middle-low range (6.7–63 mg/kg).The middle-high values are situated near areas of known mineralization and old mining sites. The legal limits for Pb (RAL = 20 mg/kg and IAL = 1000 mg/kg) are also exceeded (Table 3). An area of anomalously high Pb content in the topsoil, with values greater than 1000 mg/kg, is found in C.Postlioni.

The Sn geochemical map for topsoils shows that many surficial soils exceed RAL for Sn (1 mg/kg), especially in the village of Fiumedinisi where Sn values are above 10 mg/kg (Fig. 5E).

Figure 5F shows the distribution for Au. The values range from 0.2 to 100 µg/kg, with a mean value of 10.8 µg/kg (Table 2). The Au distribution map is quite similar to the Ag map (Fig. 5G).

The geochemical map for Ag (Fig. 5G) shows values in the range 16–1107 µg/kg, with a mean value of 116 µg/kg (Table 2). The high anomalies (up to 1107 µg/kg) occur mostly in Femmina Morta area and nearby old mining site of Tripi.

The Fe content of the topsoils has a range of values of 1.05% to 6.97% with a mean of 4.38% (Table 2). The areas where Fe shows high contents are in Femmina Morta, in the NW of Mandanici and at the south of Fiumedinisi (Fig. 5H).

Plots of Pb isotopic data

Table 4 shows Pb isotopic values for galena and for 10 selected topsoils and 6 profile samples along with Pb concentrations. The soil sites selected for Pb isotopic study are located in areas with high concentrations of As, Pb, Zn, and Sb. The letters L or R near the sample ID (Table 4) distinguish the leach and residue sample compositions, obtained by chemical preparation. The leach (L) samples represent the portion of the Pb that is readily leached from grains of soils and reflects possible anthropogenic contamination, whereas the residue (R) samples represent the residual portion of soils and reveal Pb compositions of geogenic origin (Ayuso *et al.* 2008, 2013). The field for natural compositions of the mineralized areas is defined by means of Pb isotopic ratios of galena; the compositions of residue (R) samples can be ascribed to geogenic or natural background values in samples not associated with mineralization (Fig. 6B). Galena samples FD2 and FD4 were collected in the Budali mine (Fiumedinisi); FD03A, FD03B, FD03C, FD03D in the Tripì mine (nearby Ali village) and CAL4C in the Vacco and Migliuso mine (Fig. 2). The anthropogenic field is composed by isotopic ratios of Pb in the aerosol and gasoline of Sicily island (Table 5; Monna *et al.* 1999; Fig. 6A).

Figure 7 shows the metal contents of As, Zn, Sb, Pb, Sn and Fe v. isotopic ratios of $^{206}Pb/^{207}Pb$.

Discussion

Table 6 shows for comparison statistical parameters of the soil and stream sediment trace element data. Geochemical distribution of the elements in the detailed survey of the topsoils is not always in agreement with the concentrations found in stream sediment data (De Vivo *et al.* 1993, 1998*a*). Marked differences are recorded for trace elements with low mobility in the surface environment, for example Ba, Be, Bi, Cr, Nb, Sn, V and Zr. These elements show mean values in stream sediments that are much higher than in the soils. The most striking case is for Zr with a mean value 80 times higher in stream sediments than in soils, followed by Bi (14 times) and Nb (8 times). Arsenic, Cu, Zn, Hg show a wider range of concentrations in stream sediments compared to the soils but the mean values are much higher in soils. Stream sediments represent composite samples from the catchment area upstream from the sampling site. In the stream environment, the mobility of the different elements varies considerably; low mobility trace elements can be strongly enriched in the sediments. In contrast, residual soil compositions are closely related to the bedrock lithology, from which they formed by weathering and leaching processes, and which typically may display anomalous concentrations of elements from underlying mineralization. Making comparisons with mean values from uncultivated soils (Table 2) shows that the soils have higher As, Cd, Cu, Ni, Pb, Sb, Sn, V, Zn and Hg concentrations. In fact, some of the high metal concentrations are of concern and could affect human health. Figure 3 (A–D), for example, shows that As,

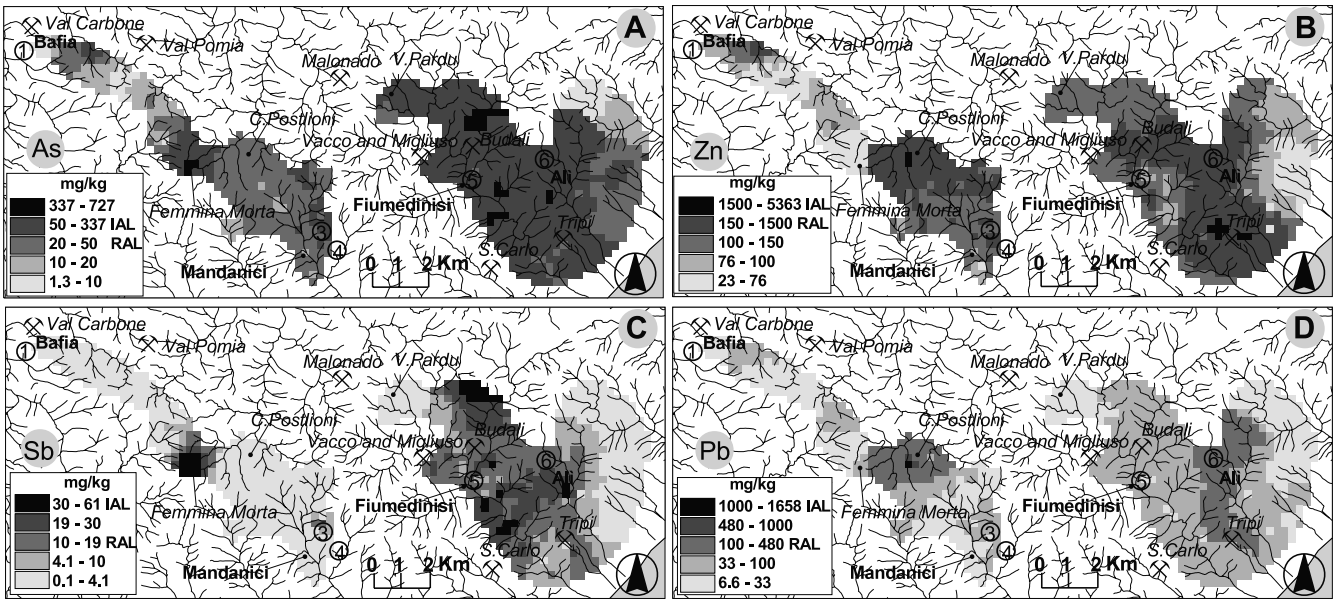

Fig. 4. Interpolated geochemical maps of As, Zn Sb and Pb (A–D). Areas of mineralization and old mining locations are also shown. For potentially toxic elements, class intervals where the upper limit corresponds to the Residential Action Limit (RAL) and/or to the Industrial Action Limit are also indicated.

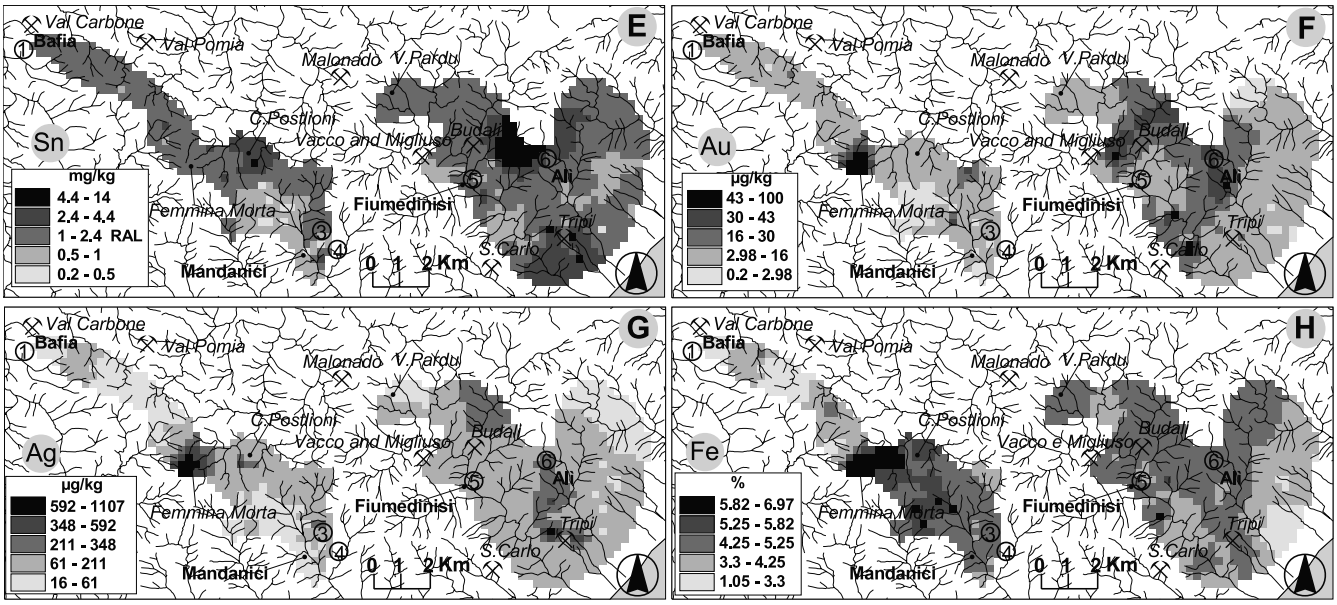

Fig. 5. Interpolated geochemical maps of Sn, Au, Ag, and Fe (E–H). Areas of mineralization and old mining locations are also shown. For potentially toxic elements, class intervals where the upper limit corresponds to the Residential Action Limit (RAL) and/or to the Industrial Action Limit IAL are also indicated.

Zn, Sb and Pb exceed limits recommended for residential and recreational areas (Table 3). Potentially harmful elements such as Cd, Hg, Sn, V (Fig. 3E–H) and Ni and Cu (not shown) exceed only the RAL. Particularly striking is the case of the As content in soils (Fig. 4A), in which *c.* 52% of samples exceed 20 mg/kg (the As RAL), and *c.* 30% exceed 50 mg/kg (the As IAL). This is relevant for both mineral exploration purposes for the identification of unknown Au resources and for environmental contamination issues. Also Sn concentrations are significant because *c.* 55% of samples exceed the RAL of 1 mg/kg (Fig. 5E). Again, regardless of the origin of these anomalously high metal contents (geogenic or anthropogenic), the elements can pose a risk to human health.

Figures 4 and 5 show the distribution patterns in topsoils of selected elements and the areas affected by high levels of toxic metal contamination. The high concentration of many of these elements is also evident in spring and surface waters (Dongarrà *et al.* 2009). Anomalous contents of As (up to 726 mg/kg), Sb (up to 61 mg/kg), Au (up to 0.1 mg/kg) and Ag (up to 1.1 mg/kg) occur in the Femmina Morta locality and between Fiumedinisi, Budali and Alì, near old mining sites. An area characterized by an Au anomaly near Femmina Morta was not detected in previous stream sediment surveys at regional or local scales (De Vivo *et al.* 1993, 1998*a*). These new findings confirm that the distribution of metal or just Au anomalies can be related to the thrust zone belt between the Aspromonte and Mela and/or Mandanici units (Fig. 2). The occurrences of Au deposits related to hydrothermal ore solutions in thrust and shearing zone systems are well known and are commonly classified as orogenic lode Au

Table 4. *Isotopic ratios of Pb from galena collected from old mining sites of Vacco and Migliuso, Tripi and Budali. Isotopic ratios of Pb leach (L) and residue (R) of topsoils and profile soils collected in the studied area*

Sample	Type	$^{206}Pb/^{207}Pb$	$^{208}Pb/^{207}Pb$	$^{208}Pb/^{206}Pb$	Pb (mg/kg)	Zn (mg/kg)	As (mg/kg)	Sb (mg/kg)	Sn (mg/kg)	Fe (%)
FD03C	Galena	1.1728	2.4596	2.0971						
CAL4C	Galena	1.1893	2.4794	2.0848						
FD03D	Galena	1.1718	2.4602	2.0995						
FD03B	Galena	1.1731	2.4574	2.0947						
FD03A	Galena	1.1727	2.4586	2.0965						
FD2	Galena	1.1767	2.4590	2.0898						
FD4	Galena	1.1738	2.4590	2.0949						
PROF1 0–20 R	Soil profile	1.2063	2.4806	2.0563						
PROF2 0–20 R	Soil profile	1.1930	2.4828	2.0811						
PROF3 0–20 R	Soil profile	1.1847	2.4774	2.0912						
PROF1 80–100 R	Soil profile	1.1954	2.4776	2.0727						
PROF2 80–100 R	Soil profile	1.1925	2.4845	2.0834						
PROF3 80–100 R	Soil profile	1.1839	2.4777	2.0928						
PEL8 R	Topsoil	1.1796	2.4641	2.0889						
PEL10b R	Topsoil	1.1954	2.4875	2.0809						
PEL8L	Topsoil	1.1737	2.4549	2.0917	95	123	186	35.6	1.50	5.16
PEL14L	Topsoil	1.1840	2.4731	2.0988	57.6	131	465	22.8	1.20	5.03
PEL39L	Topsoil	1.1787	2.4581	2.0854	52.9	154	204	22.2	1.50	4.19
PEL64L	Topsoil	1.1757	2.4603	2.0927	391	5363	142	8.56	5.60	4.67
PEL153L	Topsoil	1.1695	2.4606	2.1038	1658	2503	60.5	2.47	1.80	4.8
PEL62L	Topsoil	1.1745	2.4580	2.0929	475	3095	260	14.3	5.70	4.62
PEL55L	Topsoil	1.1828	2.4686	2.0870	255	1523	121	10.4	0.80	4.65
PEL120L	Topsoil	1.1968	2.4702	2.0640	28.3	58.3	10.7	0.29	2.10	2.75
PEL170L	Topsoil	1.1756	2.4593	2.0921	340	1835	25.7	1.99	6.40	4.82
PEL181L	Topsoil	1.1757	2.4566	2.0895	145	177	222	25.0	1.20	4.63
PROF1 0–20L	Soil profile	1.2041	2.4814	2.0608	51.2	146	32.4	0.53	2.60	5.22
PROF2 0–20L	Soil profile	1.1955	2.4822	2.0763	12.8	102	31.8	0.17	1.60	4.38
PROF3 0–20L	Soil profile	1.1799	2.4647	2.0889	59.2	152	262	21.8	0.90	4.24
PROF1 80–100L	Soil profile	1.1981	2.4873	2.0761	87.6	239	63.0	1.28	2.50	9.27
PROF2 80–100L	Soil profile	1.1928	2.4793	2.0785	15.1	120	35.6	0.15	2.00	4.9
PROF3 80–100L	Soil profile	1.1781	2.4660	2.0932	58.7	149	274	21.7	0.70	4.34

Table 5. *Isotopic ratios of Pb in aerosol and gasoline measured in the Sicily region, from Monna* et al. *(1999).*

Sample	Type	$^{206}Pb/^{207}Pb$	$^{208}Pb/^{207}Pb$
PALERMO	Aerosol	1.119	2.3991
PALERMO	Aerosol	1.118	2.3958
PALERMO	Aerosol	1.106	2.3767
PALERMO	Aerosol	1.123	2.4054
PALERMO	Aerosol	1.117	2.3993
SIRACUSA	Aerosol	1.167	2.4530
SIRACUSA	Aerosol	1.168	2.4504
CALTANISSETTA	Aerosol	1.107	2.3800
CALTANISSETTA	Aerosol	1.113	2.3873
CALTANISSETTA	Aerosol	1.126	2.4028
GELA	Aerosol	1.113	2.3896
GELA	Aerosol	1.165	2.4441
PORTO EMPEDOCLE	Aerosol	1.149	2.4243
PORTO EMPEDOCLE	Aerosol	1.149	2.4232
CATANIA	Aerosol	1.165	2.4558
CATANIA	Aerosol	1.161	2.4497
CATANIA	Aerosol	1.174	2.4536
CATANIA	Aerosol	1.168	2.4469
MESSINA	Aerosol	1.103	2.3736
MESSINA	Aerosol	1.104	2.3769
MILAZZO	Aerosol	1.119	2.3901
MILAZZO	Aerosol	1.141	2.4143
AGIP gasoline	Gasoline	1.066	2.3505
IP gasoline	Gasoline	1.084	2.3479
TEXACO (England)	Gasoline	1.059	2.3266
TESCO (England)	Gasoline	1.061	2.3299
BP (England)	Gasoline	1.062	2.3332
TOTAL (England)	Gasoline	1.066	2.3398
ESSO (England)	Gasoline	1.068	2.3399

deposits (Walshe & Cleverley 2009). The latter mineralization, which is structurally controlled and associated with extensive chemical alteration of the country rocks, is thought to have formed by transport of metals by hydrothermal-metamorphic fluid. Gold sulphide complexes can be transported by metamorphic fluids, usually structurally controlled by faulting or other structural features associated with extensive chemical alteration of the wallrocks. These fluids which remobilise silica and metals later precipitate in response to decreasing pressures and/or temperatures giving rise to the auriferous quartz veins often within igneous intrusive rocks. In this case, crustal rocks, affected by greenschist-facies metamorphism, can be the source rocks for Au mineralization associated with hydrated minerals, carbonate minerals and sulphides, and as described previously, with enrichment of metalloids (As, Sb, Sn). Gold has been very likely reprecipitated in response to the loss of the sulphide ligand (sulphidation), from the reaction with Fe in silicate and oxide minerals of the wallrock (Williams-Jones *et al.* 2009). This is reflected by the occurrence of very high Fe concentrations in soils (mean of 4.38%, Table 2) that, in the Femmina Morta and Fiumedinisi areas, reach the unusually high concentration of 6.97% (Table 2; Fig. 5H).

Environmental studies make use of Pb isotopic signatures in combination with metal concentration data to trace the origin and the extent of anthropogenic contamination. Lead has a naturally variable isotopic composition depending on both the U–Th–Pb abundance of a given reservoir and the decay schemes of the radioactive isotopes of Th and U (i.e. their half-lives). The significant difference in half-lives and the variations of U, Th and Pb contents in natural materials produced a relatively wide range of Pb isotope ratios in the different reservoirs on the Earth. Furthermore, Pb is

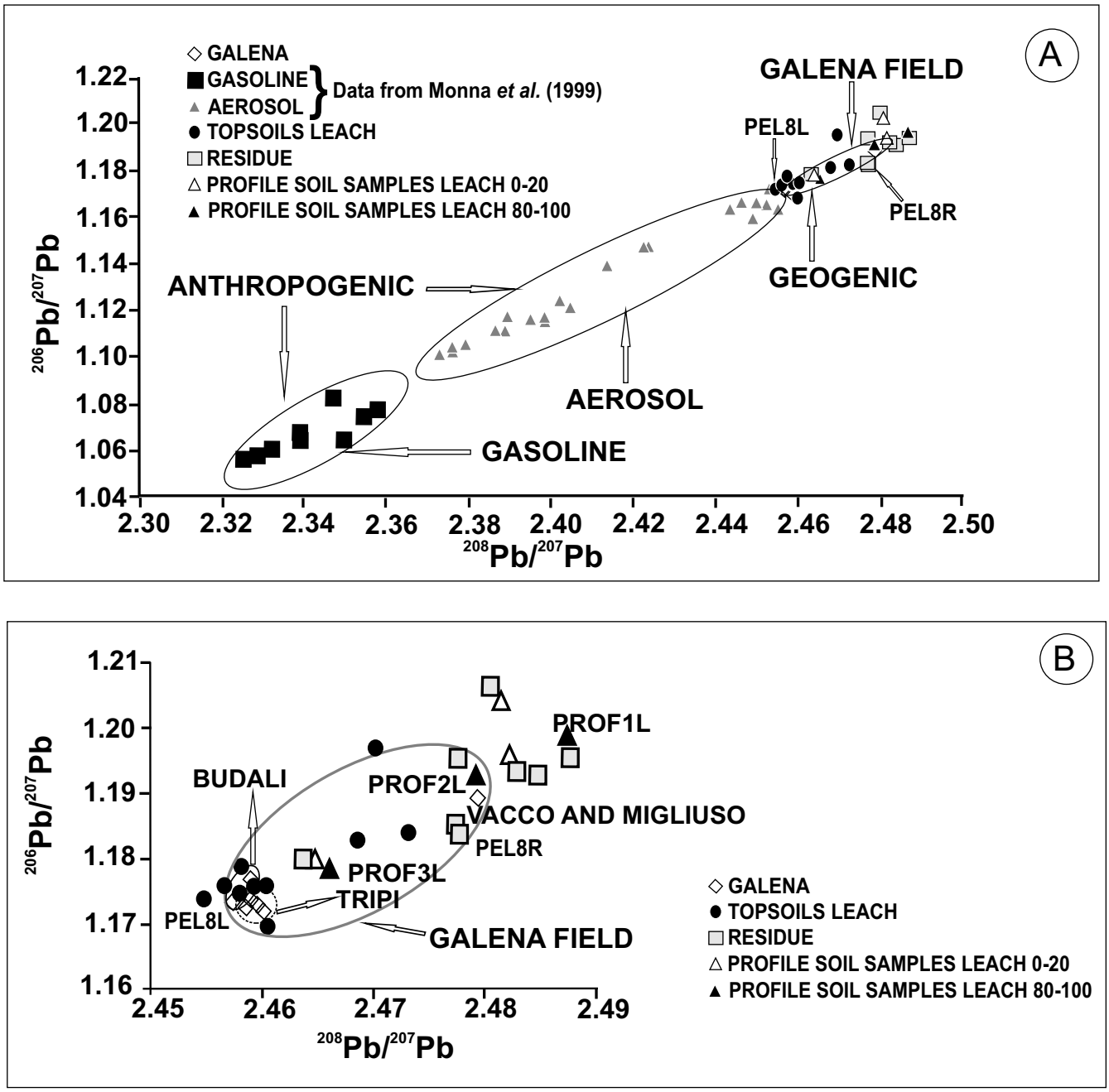

Fig. 6. (**A**) Comparison between the isotopic ratio values of selected topsoil and profile samples and galena samples (this study), which are used to establish the geogenic field. Pb isotopic ratios of fossil fuels (gasoline) and gaseous emissions in the atmosphere (aerosols) of industrial areas of Sicily (Monna *et al.*, 1999) establish the anthropogenic field. (**B**) Plot of Pb isotopic ratios. Leached and residue data are plotted for selected topsoils and profile soils.

retained in soils over time and Pb isotopes are not fractionated by environmental and industrial processes (i.e. the source retains its isotopic composition). The isotopic composition of anthropogenic Pb emitted by the combustion of leaded gasoline and, subordinately, emitted by other sources such as power plants, is controlled by the isotopic values of the ores used for the production of petrol–lead (alkyl–lead) and the materials utilized for industrial activities (Ayuso *et al.* 2008). If Pb consists of two isotopically homogeneous components, for example a natural Pb and an anthropogenic Pb component, then the isotopic ratios of natural v. anthropogenic Pb are linearly related; otherwise, a non-linear mixing trend will be observed indicating the presence of Pb derived from more than two sources (Ayuso *et al.* 2008, 2013; Tarzia *et al.* 2002).

Figure 6A and B show all measured isotopic ratios of Pb. The field for naturally occurring Pb defined by galena values (Table 4) is labelled as 'geogenic' (Fig. 6A). The natural end-member field for galena is elongated as the Pb isotopic ratio of the CAL4C sample ($^{206}Pb/^{207}Pb = 1.1893$ and $^{208}Pb/^{207}Pb = 2.4794$) (Table 5; Fig. 6A and B) differs from most galena samples. The other galena samples of the Mandanici unit have average isotopic ratios of 1.1735 for $^{206}Pb/^{207}Pb$ and 2.4590 for $^{208}Pb/^{207}Pb$ (Table 4; Fig. 6A and B). Anthropogenic fields for Pb have been obtained using the Pb isotopic ratios of fossil fuels (gasoline) and gaseous emissions in the atmosphere (aerosols) emanating from the nearby Milazzo industrial areas of Sicily. At Milazzo, 15 km north of the investigated area (Fig. 1), is one of the largest oil refineries of southern Italy (Table 5; Fig. 6A; Monna *et al.* 1999). The three isotopic fields plot along a trend indicating a possible two-end member mixing line between anthropogenic and geogenic Pb for the region. The isotopic Pb leach ratios of topsoils show a linear trend with a

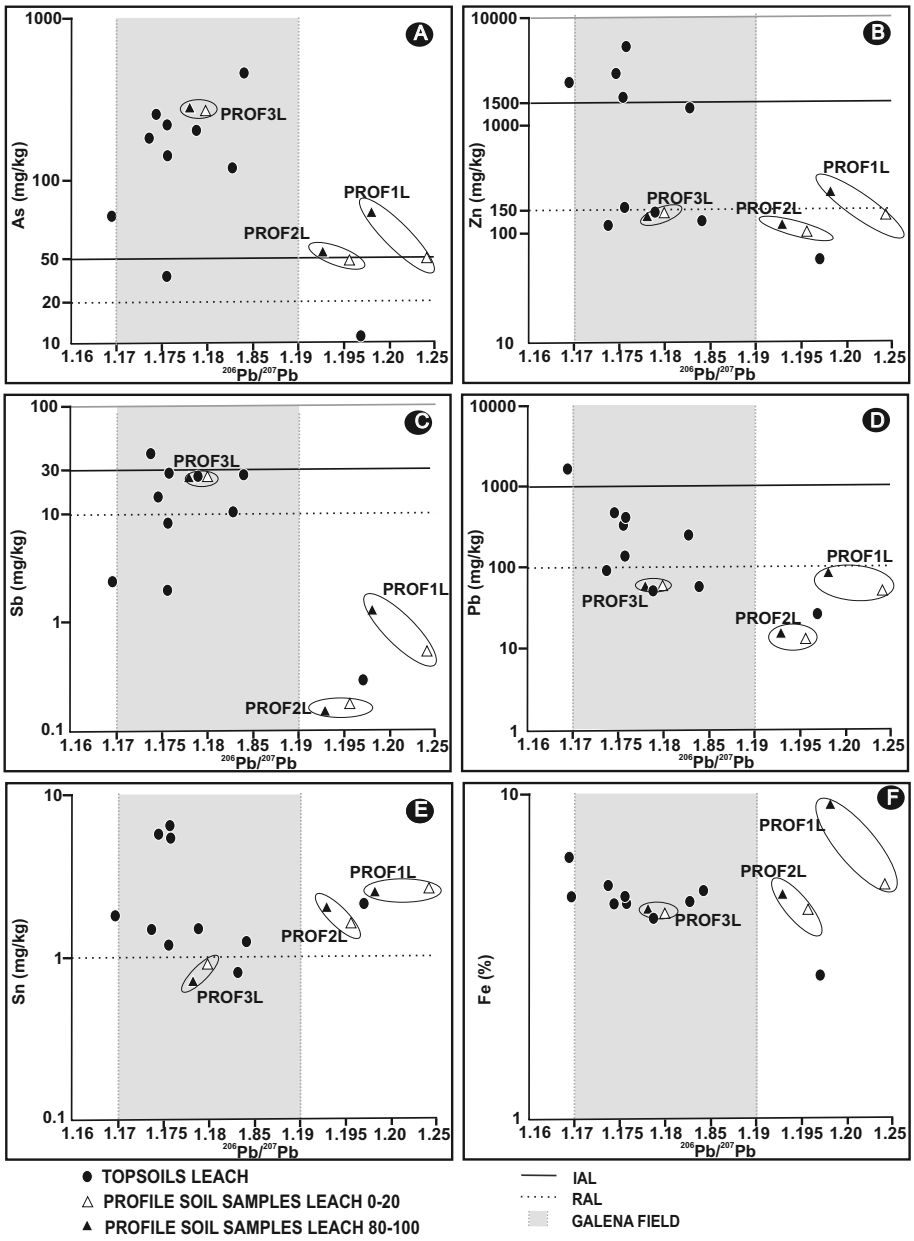

Fig. 7. Metal contents in the topsoils and in profile soil samples v. signatures of $^{206}Pb/^{207}Pb$. (**A**) As, (**B**) Zn, (**C**) Sb, (**D**) Pb, (**E**) Sn and (**F**) Fe. The shaded area is the galena field.

natural end member. The leach data indicate that most of the topsoils contain geogenic-type Pb, whereas only one topsoil (PEL8L) has a Pb isotopic ratio near the range of the aerosols composition (Monna *et al.* 1999).

The topsoil (0–20 cm) leach data from three profiles plot within or near the galena field (Fig. 6A and B), sample PROF1 being collected at C. Postlioni where the Pb concentration in soil is more than 1658 mg/kg. The leach Pb isotope ratios of three bottom profile samples (80–100 cm) also show a linear trend within the geogenic field, and confirm that the Pb isotopic composition of these soils is affected by the galena mineralization occurrence (Fig. 6B). In particular, PROF3 bottom sample has isotopic values very close to the galena from the Mandanici unit collected in the Tripi mine. The PROF2 bottom sample has isotopic values similar to galena from the Mela unit (CAL4C) collected in Vacco and Migliuso mine.

The residue Pb ratios of the PEL8R sample ($^{206}Pb/^{207}Pb = 1.1796$ and $^{208}Pb/^{207}Pb = 2.4641$; Table 4) fall in the centre of the natural galena field, close to galena CAL4C, and far from the PEL8L (leach) sample, the latter being close to the aerosol field. Lead emissions from the Milazzo petroleum refinery are a plausible source of the contamination of PEL8L. In the latter sample, Pb has a concentration of 95 mg/kg (Table 4), which is lower than the RAL.

Figure 7 shows the As, Zn, Sb, Pb, Sn and Fe contents of topsoils and profile soil samples v. the combined leach Pb isotopic signatures of $^{206}Pb/^{207}Pb$. In each plot, the dotted line indicates values exceeding the RAL, whereas the continuous line indicates values exceeding the IAL. Once again, only one sample has an As content below the IAL and only for Sn no sample exceeds the IAL. The isotopic ratios of $^{206}Pb/^{207}Pb$ of 1.17 and 1.19 mark the galena field (in gray). Almost all of the surface soils and soils collected from PROF3 have high concentrations of metals, with the $^{206}Pb/^{207}Pb$ ratios falling in the galena field. While the PROF1 and the PROF2 soils have lower Sb and As and higher Sn contents compared with PROF3 soils, their leach $^{206}Pb/^{207}Pb$ ratios fall outside the galena field. As already discussed, the PROF1 and the PROF2 leach $^{206}Pb/^{207}Pb$ and $^{208}Pb/^{207}Pb$ isotopic signatures are related to their residue Pb ratios and fall in the geogenic field. These differences could be interpreted as variations in the natural source, likely due to the hydrothermal ore solutions moving in thrust and shear zone systems.

Table 6. *Statistical parameters of the soil and stream sediment trace element*

Elements	Topsoils $n=122$ Follow-up survey			Stream Sediments $n=118$*			Stream Sediments $n=1198$**		
	Range	Mean	Std Dev	Range	Mean	Std Dev	Range	Mean	Std Dev
As (mg/kg)	1.3-727	84	122.2	10-621	80	88	10-2232	39	111
Ba (mg/kg)	16.4-974	144.6	117.6	295-973	610	109	99-1653	614	130
Be (mg/kg)	0.2-2.3	0.9	0.4	2-7.4	3.1	0.8	0.5-7.4	2.8	0.6
Bi (mg/kg)	0.05-1.4	0.4	0.2	5-23.4	5.6	2.8	5-46.8	6.8	4.1
Cd (mg/kg)	0.02-11	0.4	1.2	0.5-8	0.6	0.7	1-6.9	1.0	0.3
Ce (mg/kg)	6.9-244	67.5	41.7	64-153	91	15	27-546	107	37
Co (mg/kg)	5.6-62	24.9	9.6	10-40	22	5	1.1-80	17	7
Cr (mg/kg)	4-105	42.9	19.1	61-334	105	33	14-397	94	38
Cu (mg/kg)	6.4-169	62.8	25.3	34-168	61	22	7-212	45	18
La (mg/kg)	3.3-130	32.9	20.1	35-112	50	10	12-415	58	23
Li (mg/kg)	5.3-111	42.8	19.4	16-85	42	17	5-308	66	30
Mo (mg/kg)	0.19-4.4	1.2	0.5	1-4.3	1.3	0.8	1-21	1.7	1.3
Nb (mg/kg)	0.09-11.6	2.3	2.4	12-30	18	3	5-47	20	6
Ni (mg/kg)	10.7-136	48.1	17.9	29-159	62	21	2-653	54	29
Pb (mg/kg)	6.6-1658	65.8	160.4	5-1150	46	107	5-1365	39	51
Sb (mg/kg)	0.1-61	7.6	12.2	5-29	6	4	5-107	8	8
Sn (mg/kg)	0.2-14.5	1.5	1.6	5-18	6	3	5-82	7	4
V (mg/kg)	11-132	54.6	26.3	97-164	130	16	21-289	119	34
Zn (mg/kg)	23.4-5363	241	614.4	71-2032	203	269	27-5433	138	180
Zr (mg/kg)	0.2-17.3	3.1	3.7	111-475	239	60	82-2388	270	124
Ag (µg/kg)	16-1107	115.7	142.8	100-5100	200	500	100-900	500	0.06
Au (µg/kg)	0.2-100	10.7	14.9	3-1005	34	167	5-1040	9	34
Hg (µg/kg)	3.7-1564	169.4	268.6	20-300	38	53	20-4000	74	216

Data from *De Vivo *et al.* (1993) and **De Vivo *et al.* (1998*a*).

Conclusion

This paper reports a geochemical investigation carried out on topsoils and vertical profiles distributed over an area of 250 km^2 in the eastern-central Peloritani Mountains northeastern Sicily. The main results can be summarized as follow:

- Most of the soils show high concentrations of harmful elements exceeding both the RAL and IAL like As, Zn, Sb and Pb; other elements like Cd, Hg, Sn, V, Ni and Cu exceed only the RAL.
- Of particular concern are: As contamination because *c.* 52% of soils exceed 20 mg/kg (the As RAL), and *c.* 30% exceed 50 mg/kg (the As IAL) and Sn contamination because *c.* 55% of samples exceed the RAL of 1 mg/kg.
- Areas affected by topsoils high contamination levels are shown by geochemical maps produced for selected toxic elements.
- Barium, Be, Bi, Cr, Nb, Sn, V and Zr show mean values in stream sediments that are much higher than in the soils. Arsenic, Cu, Zn, Hg show a wider range of concentrations in stream sediments compared to the soils, with the mean values much higher in soils.
- Two anomalous areas have been detected: the larger, located between the Fiumendinisi, Budali and Ali villages, and the other between C.Postlioni and Femmina Morta. The latter, was not detected by previous surveys and represents an intriguing new result.
- Ratios of $^{206}Pb/^{207}Pb$ v. $^{208}Pb/^{207}Pb$ isotopes measured in selected soils, in profile samples, and in galena show that the leached fraction reflects geogenic contamination, related to the presence of sulphide and sulphosalt rock-forming minerals outcropping in the area.
- The correlation between metal contents in topsoils v. the combined leach $^{206}Pb/^{207}Pb$ ratios confirms that the Pb sources are sulphide minerals (galena) from hydrothermal ore solutions moving along thrust and shear zone systems.
- The anomalously high metal contents can almost be totally attributed to metals derived from mineralized occurrences, and mines, and as a legacy of mining. Only a small to negligible contribution is caused by the discharge into the atmosphere by the nearby Milazzo oil refinery.

Acknowledgements and Funding

The research results discussed in the paper have been obtained during the activities of the first author (Antonio Cosenza) as a PhD student of the PhD Programme "Turismo, Territorio and Ambiente" of the University of Messina (Italy). The isotopic investigations have been obtained at USGS (United States Geological Survey) in Reston (VA, USA) within a collaboration agreement between Prof. B. De Vivo (Univ. di Napoli Federico II) and Dr. R. Ayuso and Dr. N. Foley (USGS).

References

Amodio-Morelli, L., Bonardi, G., Colonna, V. *et al*. 1976. L'Arco Calabro-Peloritano nell'orogene Appenninico- Maghrebide. *Memorie- Società Geologica Italiana*, **17**, 1–60.

Atzori, P. 1968. Studio geo-petrografico dell'affioramento mesozoico di Alì Terme (Messina). *Accademia Gioenia di Scienze Naturali in Catania*, **20**, 134–172.

Atzori, P., Cirrincione, R., Del Moro, A. & Pezzino, A. 1994. Structural, metamorphic and geochronologic features of the Alpine event in the south-eastern sector of the Peloritani Mountains (Sicily). *Periodico di Mineralogia*, **63**, 113–125.

Ayuso, R.A., Foley, N. & Lipfert, G. 2008. Lead isotopes as monitors of anthropogenic and natural sources affecting the superficial environment. *In*: De Vivo, B., Belkin, H.E. & Lima, A. (eds) *Environmental Geochemistry: Site Characterization, Data Analysis and Case Histories*. Elsevier, Amsterdam.

Ayuso, R.A., Foley, N., Seal, R., Bove, M., Civitillo, D., Cosenza, A. & Grezzi, G. 2013. Lead isotope evidence for metal dispersal at the Callahan Cu-Zn-Pb mine: Goose Pond tidal estuary (Maine, USA). *Journal of Geochemical Exploration*, **126–127**, 1–22.

Bonardi, G., Caggianelli, A., Critelli, S. *et al*. 2004. *Geotraverse Across the Calabria-Peloritani Terrane (Southern Italy)*. Field Trip Guide Book - P66, 32nd International Geological Congress IUGS, Florence, 20–28 August, APAT 1–60.

Bonardi, G., Compagnoni, R., Del Moro, A., Macaione, E., Messina, A. & Perrone, V. 2008. Rb-Sr age constraints on the Alpine metamorphic overprint in the Aspromonte Nappe (Calabria-Peloritani Composite Terrane, Southern Italy). *Bollettino della Società Geologica Italiana*, **127**, 173–190.

Bonardi, G., De Vivo, B., Giunta, G., Lima, A., Perrone, V. & Zuppetta, A. 1982. Mineralizzazioni dell' arco calabro-peloritano; ipotesi genetiche e quadro evolutivo. *Bollettino della Società Geologica Italiana*, **101**, 141–155.

Bonardi, G., Giunta, G., Messina, A., Perrone, V. & Russo, S. 1996. *The Calabria-Peloritani Arc and Its Correlation With Northern Africa and Southern Europe*. Field Trip Guidebook – 6th Field Meeeting IGCP Project 276, Newsletter, **6**, 27–90.

Caire, A., Duee, G. & Truillet, R. 1965. La Chaine calcaire des Monts Péloritains (Sicile). *Bulletin de la Société Géologique de France*, **7**, 881–888.

Carbone, S., Messina, A. & Lentini, F. 2008. *Note Illustrative della Carta Geologica d'Italia alla Scala 1:50.000*. Foglio 601 Messina-Reggio di Calabria- Servizio Geologico d'Italia - APAT, 1-179. S.EL.CA., Florence, Italy.

Carbone, S., Messina, A., Lentini, F. & Macaione, E. 2011. *Note Illustrative della Carta Geologica d'Italia alla scala 1:50000*. Foglio 587-600 Milazzo-Barcellona P.G. ISPRA, 1-262. S.EL.CA., Florence, Italy.

Cecca, F., Critelli, S., De Capoa, P., Messina, A. & Perrone, V. 2002. Nouvelle datation et intérpretation de la succession sédimentaire de la Fiumara Sant'Angelo (Monts Péloritains, Italie méridionale): Conséquences pour la paléogéographie mésozoique de la Méditerranée centrale. *Bulletin de la Société Géologique de France*, **173**, 77–90.

Cheng, Q. 2003. *GeoData Analysis System (GeoDAS) for Mineral Exploration and Environmental Assessment, User's Guide (GeoDAS Phase III)*. York University, Toronto, Ontario, Canada.

Compagnoni, R., Borghi, A., Messina, A. & Nutarelli, F. 1998. Metamorfismo eclogitico nell'Arco Calabro-Peloritano: un evento Varisico precoce o Pre-Varisico. *Atti 79° Congresso Nazionale Società Geologica Italiana, vol. B*, 325–326, Palermo.

Connor, J.J. & Shacklette, H.T. 1975. *Background Geochemistry of Some Rocks, Soils, Plants, and Vegetables in the Conterminous United States. Statistical Studies in Field Geochemisty*. U.S Geological Survey Professional Paper **574-F**.

Decreto Legislativo 2006. 3 April, n. 152 (D. Lgs 152/06). *Norme in materia ambientale. Gazzetta Ufficiale della Repubblica Italiana*, **88**. Supplemento Ordinario n. 96, del 14 Aprile 2006.

De Gregorio, S., Rotolo, S.G. & Villa, I.M. 2003. Geochronology of the medium to high grade metamorphic units of the Peloritani Mountains, Sicily. *International Journal of Earth Sciences*, **92**, 852–872.

De Stefani, C. 1911. Il Paleozoico inferiore di Alì nel messinese. *Atti Società Toscana. Scienze Naturali*, **20**, 21–25.

De Vivo, B. 1982. Mineral resources of the Calabria-Peloritani Arc: Genetic aspects in the evolution of the Arc. *Earth Evolution Sciences*, **3**, 187–196.

De Vivo, B., Lima, A., Catalano, G. & Chersicla, A. 1993. Detailed geochemical survey in the Peloritani Arc. (northeastern Sicily, Italy): Evidence of gold anomalies. *Journal of Geochemical Exploration*, **46**, 309–324.

De Vivo, B., Messina, A., Belkin, H.E., Doughten, M.W., Fedele, L. & Lima, A. 1998*a*. Behaviour of gold anomalies in stream sediments of Peloritani Mountains (north-eastern Sicily, Italy). *Explore*, **98**, 5–11.

De Vivo, B., Sava, A., Villani, V. & Messina, A. 1998*b*. Cartografia geochimica dei Monti Peloritani (Sicilia). *In*: *Monografia Memorie Descrittive della Carta Geologica d'Italia*. Servizio Geologico Nazionale, LV, 33–93.

Dongarrà, G., Manno, E., Sabatino, G. & Varrica, D. 2009. Geochemical characteristics of waters in mineralised area of Peloritani Mountains (Sicily, Italy). *Applied Geochemistry*, **24**, 900–914.

Ferla, P. & Meli, C. 2007. Petrogenesis of tourmaline rocks associated with Fe-carbonate–graphite metapelite, metabasite and stratabound polymetallic sulphide mineralisation, Peloritani Mountains, Sicily, Southern Italy. *Lithos*, **99**, 266–288.

Guerrera, F., Martín-Algarra, A. & Perrone, V. 1993. Late Oligocene-Miocene syn- late-orogenic successions in Western and Central Mediterranean Chains from the Betic Cordillera to the Southern Apennines. *Terra Nova*, **5**, 525–544.

Lima, A., De Vivo, B., Cicchella, D., Cortini, M. & Albanese, S. 2003. Multifractal IDW interpolation and fractal filteringmethod in environmental studies: An application on regional stream sediments of Campania region (Italy). *Applied Geochemistry*, **18**, 1853–1865.

Macaione, E., Messina, A., Bonanno, R. & Carabetta, M.T. 2010. An Itinerary through Proterozoic to Holocene rocks in the North-Eastern Peloritani Mts. (Southern Italy). *Italian Geological Society -Young Section, 1st National Congress - Geology, Culture and Flavors of Sicily, Geological Field Trip*, **2**, 1–98.

Martín-Algarra, A., Messina, A., Perrone, V., Russo, S., Maate, A. & Martín-Martín, M. 2000. A lost realm in the Internal Domains of the Betic-Rifian Orogen: Evidence from Oligo-Aquitanian conglomerates and consequences for Alpine geodynamic evolution. *Journal of Geology*, **108**, 447–467.

Messina, A. 1996. The Aspromonte Unit P-T-time path (Southern Calabria-Peloritani Arc, Italy). *Plinius*, **16**, 152–154.

Messina, A., Compagnoni, R., Nutarelli, F. & Corsaro, E. 1998. *The tectono-metamorphic history of the Piraino epi-metamorphic complex (North-Western Peloritani Mountains.)*. Atti 79° Congresso Nazionale Società Geologica Italiana, vol. B, 573–576, Palermo, Italy.

Messina, A., Compagnoni, R., Russo, S., De Francesco, A.M. & Giacobbe, A. 1990. Alpine metamorphic overprint in the Aspromonte Nappe of northeastern Peloritani Mts. (Calabria-Peloritani Arc, Southern Italy). *Bollettino della Società Geologica Italiana*, **109**, 655–673.

Messina, A., Giacobbe, A., Perrone, V. & De Francesco, A.M. 1997. The Mela Unit: A new medium grade metamorphic unit in the Peloritani Mountains. (Calabrian-Peloritan Arc, Italy). *Bollettino della Società Geologica Italiana*, **115**, 16.

Messina, A., Lentini, F., Macaione, E., Carbone, S. & Doherty, A. 2013. *Tectono-stratigraphic evolution of the Southern Sector of the Calabria-Peloritani Chain: State of knowledge*. 86° Congresso Nazionale della Società Geologica Italiana - Arcavacata di Rende (CS), 2012, **5**, 163, http://doi.org/10.3301/GFT.2013.04

Messina, A., Somma, R., Macaione, E., Carbone, G. & Careri, G. 2004. Peloritani continental crust composition (Southern Italy): Geological and petrochemical evidence. *Bollettino della Società Geologica Italiana*, **123**, 405–441.

Micheletti, F., Barbey, P., Fornelli, A., Piccarretta, G. & Deloule, E. 2007. Latest Precambrian to Early Cambrian U-Pb zircon ages of augen gneisses from Calabria (Italy), with inference to the Alboran microplate in the evolution of the peri-Gondwana terranes. *International Journal of Earth Science*, **96**, 843–860.

Monna, F., Aiuppa, A., Varrica, D. & Dongarrà, G. 1999. Pb isotope composition in lichens and aerosol from Eastern Sicily: Insights into the regional impact of volcanoes on the environment. *Environmental Science & Technology*, **33**, 2517–2523.

Ogniben, L. 1960. Nota illustrativa dello schema geologico della Sicilia nord-orientale. *Rivista Mineralogica Siciliana*, **11**, 183–212.

Perrone, V., Martín-Algarra, A., Critelli, S. *et al*. 2006. 'Verrucano' and 'Pseudoverrucano' in the central-western Mediterranean Alpine chains. *In*: Chalouan, A. & Moratti, G. (eds) *Tectonics of the Western Mediterranean and North Africa*. Geological Society, London, Special Publications, **262**, 1–43, http://doi.org/10.1144/GSL.SP.2006.262.01.01

Plant, J.A., Klaver, G., Locutura, J., Salminen, R., Vrana, K. & Fordyce, F.M. 1996. *Forum of European Geological Surveys (FOREGS) Geochemistry Task Group 1994–1996 Report*. British Geological Survey (BGS) Technical Report **WP//95/14**.

Saccà, C., Saccà, D., Nucera, P., De Fazio, A. & D'urso, D. 2007. Geochemical and mineralogical features of the polymetallic deposit from Alì (NE Sicily, Italy). *Atti dell'Accademia Peloritana dei Pericolanti Classe di Scienze Fisiche, Matematiche e Naturali*, **85**, http://doi.org/10.1478/C1A0701009

Saccà, C., Saccà, D., Nucera, P. & Somma, R. 2003. Gold-bearing polymetalliferous mineralization in the Central Peloritani Mountains. (NE Sicily, Italy). *Bollettino della Società Geologica Italiana*, **122**, 503–509.

Salminen, R., Tarvainen, T., Demetriades, A. *et al*. 1998. FOREGS Geochemical Mapping Field Manual. *Geological Survey of Finland, Espoo, Guide 47*, 36. Available from http://tupa.gtk.fi/julkaisu/opas/op_047.pdf

Shacklette, H.T. & Boerngen, J.G. 1984. *Element Concentrations in Soils and Other Surficial Materials of the Conterminous United States*. U.S. Geological Survey Professional Paper 1270, 105.

Somma, R., Messina, A. & Mazzoli, S. 2005*a*. Syn-orogenic extension in the Peloritani Alpine Thrust Belt (NE Sicily, Italy): Evidence from the Alì Unit. *Comptes Rendus Geosciences*, **337**, 861–871.

Somma, R., Messina, A. & Perrone, V. 2005*b*. The Cambrian to Aquitanian geological record of the Longi-Taormina Unit (Calabria-Peloritani Arc, Southern Italy): Geodynamic implications. *Geodinamica Acta*, **18**, 417–430.

Tarzia, M., De Vivo, B., Somma, R., Ayuso, R.A., McGill, R.A.R. & Parrish, R.R. 2002. Anthropogenic vs. natural pollution: An environmental study of an industrial site under remediation (Naples, Italy). *Geochemistry: Exploration, Environment, Analysis*, **2**, 45–56.

Walshe, J.L. & Cleverley, J.S. 2009. Gold deposits: Where, when and why. *Elements*, **5**, 288.

Williams-Jones, A.E., Bowell, R.J. & Migdisov, A.A. 2009. Gold in solution. *Elements*, **5**, 281–287.

Xu, Y. & Cheng, Q. 2001. A fractal filtering technique for processing regional geochemical maps for mineral exploration. *Geochemistry: Exploration, Environment, Analysis*, **1**, 147–156.